

Dear Dr. Emilio Marañón,

Thank you very much for your kind notice with regard to our manuscript (bg-2014-554) entitled “Effects of CO₂ and iron availability on *rbcL* gene expression in Bering Sea diatoms”.

As shown below, we have modified the manuscript according to helpful comments from you and the reviewer #1. In the revised manuscript, the modified places were shown in red color.

Other eukaryotes consisted of haptophytes, pelagophytes, dictyochophytes, dinoflagellates, and diatoms which could be assigned to centrics and pennates. "Other eukaryotes consisted of haptophytes, pelagophytes, dictyochophytes, dinoflagellates, and diatoms which could not be assigned to centrics and pennates." This sentence still does not make sense, giving preceding material. There is an entire previous section on assignments to centric and pennate diatoms. I think (maybe) the authors mean:

We have amended the sentence as follows:

Line 353, “could be assigned to” → “could not be assigned to”

*"Thus, one possible mechanism underlying the reduction of diatom *rbcL* transcription observed in our study" The authors did not measure transcription (the process of generating transcripts). They measured transcripts, the net pool that results from the opposing processes of transcription and transcript degradation. We know that in many circumstances transcript stability has a major influence on transcript pools. This error occurs multiple times through the manuscript and should be corrected.*

We have corrected the words as follows:

Line 20, “expression” → “transcript abundance”

Line 98, “transcription” → “transcripts”

Line 480, “transcription” → “transcript abundance”

Line 504, “transcription” → “transcripts”

Line 523, “transcription” → “transcripts”

In addition, the following parts were also amended in the revised manuscript.

Lines 244 and 844, “1-*D*” → “*D*” (Previous notation was a mistake)

Line 469, “diatom” → “diatoms”

Line 557, “Conclusion” → “Conclusions”

Yours sincerely,

Hisashi Endo, Ph.D.

Faculty of Environmental Earth Science

Hokkaido University

North 10 West 5, Kita-ku, Sapporo

Hokkaido 060-0810, Japan

1 **Abstract**

2 Iron (Fe) can limit phytoplankton productivity in approximately 40% of the global
3 ocean, including high-nutrient, low-chlorophyll (HNLC) waters. However, there is little
4 information available on the impact of CO₂-induced seawater acidification on natural
5 phytoplankton assemblages in HNLC regions. We therefore conducted an on-deck
6 experiment manipulating CO₂ and Fe using Fe-deficient Bering Sea waters during the
7 summer of 2009. The concentrations of CO₂ in the incubation bottles were set at 380
8 and 600 ppm in the non-Fe-added (control) bottles and 180, 380, 600, and 1000 ppm in
9 the Fe-added bottles. The phytoplankton assemblages were primarily composed of
10 diatoms followed by haptophytes in all incubation bottles as estimated by pigment
11 signatures throughout the 5 (controls) or 6 (Fe-added treatments) days incubation period.
12 At the end of incubation, the relative contribution of diatoms to chlorophyll *a* biomass
13 was significantly higher in the 380 ppm CO₂ treatment than in the 600 ppm treatment in
14 the controls, whereas minimal changes were found in the Fe-added treatments. These
15 results indicate that, under Fe-deficient conditions, the growth of diatoms could be
16 negatively affected by the increase in CO₂ availability. To further support this finding,
17 we estimated the expression and phylogeny of *rbcL* (which encodes the large subunit of
18 RubisCO) mRNA in diatoms by quantitative reverse transcription PCR and clone
19 library techniques, respectively. Interestingly, regardless of Fe availability, the
20 **transcript abundance** of *rbcL* decreased in the high CO₂ treatments (600 and 1000 ppm).
21 The present study suggests that the projected future increase in seawater *p*CO₂ could
22 reduce the RubisCO transcription of diatoms, resulting in a decrease in primary
23 productivity and a shift in the food web structure of the Bering Sea.

24

25 **1. Introduction**

26 The atmospheric CO₂ concentration has risen from a pre-industrial level of
27 approximately 280 ppm to the present level of approximately 400 ppm (WMO, 2013).
28 Since the industrial revolution, the ocean has absorbed about one-third of CO₂ emitted
29 by human activity (Sabine et al., 2004). It is predicted that the atmospheric CO₂
30 concentration could reach more than 700 ppm by the end of the 21st century (Meehl et
31 al, 2007), driving a surface seawater pH decrease of 0.3–0.4, the so-called “ocean

32 acidification” (Caldeira and Wickett, 2003). Such a rapid decrease in seawater pH has
33 most likely not occurred for at least millions of years in the earth’s history (Pearson and
34 Palmer, 2000). Therefore, it has been suggested that these predicted changes in seawater
35 carbonate chemistry would have enormous impacts on the health and function of marine
36 organisms (Raven et al., 2005).

37 In the last decade, numerous studies have been performed to evaluate the impacts of
38 ocean acidification on marine phytoplankton. In laboratory incubation experiments
39 using individual species (a single strain), the response of phytoplankton to increased
40 CO₂ levels differed among phytoplankton species, possibly depending on their ability to
41 assimilate carbon (Riebesell and Tortell, 2011; Collins et al., 2014). In the natural
42 environment, these taxon-specific differences in CO₂ response can cause a shift in the
43 phytoplankton community composition (Engel et al., 2008; Meakin and Wyman, 2011;
44 Endo et al., 2013) and subsequent changes in ocean trophic structures and
45 biogeochemical cycles (Riebesell et al., 2007; Yoshimura et al., 2013). However, the
46 current understanding of the effects of elevated CO₂ on marine phytoplankton is still
47 insufficient at the community level.

48 In terms of physiology, CO₂ is fixed by the carboxylation enzyme ribulose
49 bisphosphate carboxylase/oxygenase (RubisCO) in the Calvin-Benson-Bassham (CBB)
50 cycle. In general, the half-saturation constant of the enzyme ranges between 20 and 70
51 μmol kg⁻¹ CO₂ (Badger et al., 1998), whereas the ambient seawater CO₂ levels are
52 between 10 and 25 μmol kg⁻¹. Therefore, the present CO₂ concentration could be
53 insufficient to ensure effective RubisCO carboxylation. The progression of ocean
54 acidification could enhance photosynthetic carbon fixation in marine phytoplankton by
55 increasing CO₂ availability.

56 Recent advances in molecular biology techniques have enabled us to examine the
57 taxon-specific responses to environmental changes by quantifying functional gene
58 expression in natural phytoplankton assemblages. For example, John et al. (2007a)
59 developed a suite of quantitative reverse transcription PCR (qRT-PCR) assays to
60 quantify *rbcL* (gene encoding the large subunit of RubisCO) mRNA in *Synechococcus*,
61 haptophytes, and heterokonts including diatoms. John et al. (2007b) demonstrated a
62 strong negative correlation between diatom-specific *rbcL* mRNA abundance and

63 seawater $p\text{CO}_2$ in the Mississippi River plume, suggesting that diatoms were
64 responsible for the greatest drawdown in seawater $p\text{CO}_2$. In addition, positive
65 correlations between diatom-specific *rbcL* transcripts and light-saturated photosynthetic
66 rates (P_{max}) in seawater were reported (Corredor et al., 2004; John et al., 2007b). These
67 results suggest that *rbcL* expression in diatoms could be used to estimate the
68 photosynthetic carbon-fixation capacity of natural phytoplankton assemblages.
69 Therefore, quantification of clade-specific *rbcL* transcripts can be used to assess the
70 physiological photosynthetic responses of individual phytoplankton taxa to
71 environmental changes.

72 The oceanic Bering Sea investigated in this study is an HNLC region (Banse and
73 English, 1999), where low iron (Fe) availability limits phytoplankton growth and nitrate
74 utilization, so surface chlorophyll *a* (Chl *a*) concentrations usually remain low in the
75 summer (Suzuki et al., 2002). Despite the low phytoplankton biomass, the oceanic
76 domain has the greatest amount of total primary and secondary production in the Bering
77 Sea (Springer et al., 1996). Suzuki et al. (2002) reported that diatoms were the dominant
78 phytoplankton group in the oceanic regions of the Bering Sea in the summer. In
79 addition, Takahashi et al. (2002) showed that diatoms had the greatest contribution in
80 the sinking particles in the area. However, less is known about the combined effects of
81 ocean acidification and Fe enrichment on diatoms in such HNLC regions. In addition,
82 there are no reports on the effects of CO_2 and Fe availability on *rbcL* transcription of
83 natural diatom community in HNLC regions.

84 The purpose of this study is to clarify the responses of phytoplankton, especially
85 diatoms, to CO_2 enrichment under Fe-depleted and Fe-replete conditions in the Bering
86 Sea basin using on-deck bottle incubation. Recently, Sugie et al. (2013) reported
87 changes in phytoplankton biomass and nutrient stoichiometry in this experiment. They
88 showed that Chl *a* biomass decreased with increased CO_2 levels only in Fe-depleted
89 treatments, suggesting that Fe deficiency and increased CO_2 synergistically reduced the
90 growth of phytoplankton in the study area. In addition, Yoshimura et al. (2014)
91 demonstrated that the net production of particulate organic carbon (POC) and total
92 organic carbon (TOC) decreased under high CO_2 levels only in the Fe-limited
93 treatments, whereas those in the Fe-replete treatments were insignificantly different.

94 These studies suggest that the increase in CO₂ could have negative impacts on
95 phytoplankton growth and/or organic-matter production especially under Fe-depleted
96 conditions. However, the molecular mechanisms of photosynthetic carbon assimilation
97 in phytoplankton assemblages were not mentioned in the previous studies. Therefore, in
98 the present paper, we primarily focused on changes in *rbcL* transcripts in diatoms with
99 different CO₂ and/or Fe availability.

100

101 **2. Materials and Methods**

102 **2.1 Experimental setup**

103 The study was carried out aboard the R/V *Hakuho Maru* (JAMSTEC) during the
104 KH-09-4 cruise in September 2009. The water samples for incubation were collected
105 from 10 m depth at a station (53° 05' N, 177° 00' W) in the Bering Sea on 9 September
106 with acid-cleaned Niskin-X bottles attached to a CTD-CMS system. A total of 300 L of
107 seawater was poured into six 50 L polypropylene carboys through acid-clean silicon
108 tubing with a 197 µm mesh Teflon net to remove large particles. Subsamples were taken
109 from each carboy and poured into triplicate acid-cleaned 12 L polycarbonate bottles
110 (total 18 bottles) for incubation. Initial samples were collected from each carboy. All
111 sampling was carried out using a trace-metal clean technique to avoid any trace metal
112 contamination. Prior to incubation, FeCl₃ solutions (5 nmol L⁻¹ in final concentration)
113 were added to 12 bottles in order to reduce Fe limitation for the phytoplankton
114 communities. The CO₂ levels in the incubation bottles were manipulated by injecting
115 CO₂ controlled dry air purchased from a commercial gas supply company
116 (Nissan-Tanaka Co., Japan). The air mixtures were passed through 47 mm PTFE filters
117 (0.2 µm pore size, Millipore) before being added to the incubation bottles. The detailed
118 procedures for trace metal clean techniques were described in Yoshimura et al. (2013).
119 The CO₂ concentrations were set at 380 and 600 ppm for the non-Fe-added (control)
120 bottles (hereafter referred to as 'C-380' and 'C-600', respectively), and 180, 380, 600,
121 and 1000 ppm for the Fe-added bottles (hereafter referred to as 'Fe-180', 'Fe-380',
122 'Fe-600', and 'Fe-1000', respectively). Incubation was performed on deck in
123 temperature-controlled water-circulating tanks for 5 (controls) or 6 (Fe-added
124 treatments) days at the in situ temperature (8.2°C) and 50% surface irradiance adjusted

125 by natural density screens. The sampling opportunities for each parameter are shown in
126 Table S1.

127

128 **2.2 Carbonate chemistry, nutrients, and Chl *a***

129 The detailed methodology and basic chemical and biological parameters were
130 reported in Sugie et al. (2013). In brief, during the incubation experiment, samples were
131 collected from the incubation bottles for dissolved inorganic carbon (DIC), total
132 alkalinity (TA), nutrients, and Chl *a* determination. DIC and TA concentrations were
133 measured with a total alkalinity analyzer using the potentiometric Gran plot method
134 (Kimoto Electric) following Edmond (1970). The levels of $p\text{CO}_2$ and pH were
135 calculated from the DIC and TA using the CO2SYS program (Lewis and Wallace,
136 1998). Concentrations of nitrate plus nitrite, nitrite, phosphate, and silicic acid were
137 measured using a QuAATro-2 continuous-flow analyzer (Bran+Luebbe). The
138 concentration of total dissolved Fe (TD-Fe) was determined by a flow-injection method
139 with chemiluminescence detection (Obata et al., 1993). Chl *a* concentrations were
140 determined with a Turner Design fluorometer (model 10-AU) with the non-acidification
141 method (Welschmeyer, 1994).

142

143 **2.3 HPLC and CHEMTAX analyses**

144 Samples for high-performance liquid chromatography (HPLC) pigment analysis
145 were collected on days 3 and 5 for the control treatments and on days 2, 4, and 6 for the
146 Fe-added treatments. Water samples (400–1000 mL) were filtered onto GF/F filters
147 under gentle vacuum (< 0.013 MPa) and stored in liquid nitrogen or a deep freezer
148 (-80°C) until analysis. HPLC pigment analysis was performed following the method of
149 Endo et al. (2013).

150 To estimate the temporal changes in phytoplankton community structure during
151 incubation, the CHEMTAX program (MacKey et al., 1996) was used following Endo et
152 al. (2013). Briefly, optimal initial ratios were obtained following the method of Latasa
153 (2007). Matrix A was obtained from Suzuki et al. (2002) (Table S2), who examined
154 phytoplankton community compositions in the Bering Sea. Matrices B, C, and D were
155 also prepared to determine the optimal pigment/Chl *a* ratios (Table S2). The pigment

156 ratios of Matrices B and C were double and half the Matrix A ratio, respectively. For
157 Matrix D, values of 0.75, 0.5, and 0.25 for dominant (rank in high pigment/Chl *a* ratio:
158 1–5), secondary (rank: 6–10), and minor (rank: 11–15) pigments, respectively, were
159 multiplied by each pigment ratio of Matrix A. We averaged the successive convergent
160 ratios after the 10 runs among the 4 matrices to identify the most promising initial
161 pigment ratios. The calculated final pigment/Chl *a* ratios in both the control and
162 Fe-added treatments (Table S3) were within the range of values reported in Mackey et
163 al. (1996), Wright and van den Enden (2000), and Suzuki et al. (2002).

164

165 **2.4 qPCR and qRT-PCR**

166 Water samples for DNA and RNA analyses were collected on days 3 and 5 for the
167 control treatments and on days 2, 4, and 6 for the Fe-added treatments. DNA samples
168 (400–500 mL) were collected onto 25 mm, 0.2 μm pore size polycarbonate Nuclepore
169 filters (Whatman) with gentle vacuum (< 0.013 MPa) and stored in liquid nitrogen or a
170 deep freezer at -80°C until analysis. DNA extraction was performed following the
171 method of Endo et al. (2013). Extracted DNA pellets were resuspended in 100 μL of 10
172 mM Tris-HCl buffer (pH 8.5).

173 For RNA analysis, seawater samples (400–500 mL) were filtered onto 25 mm, 0.2
174 μm pore size polycarbonate Nuclepore filters (Whatman) with gentle vacuum (< 0.013
175 MPa) and stored in 1.5 mL cryotubes previously filled with 0.2 g of muffled 0.1 mm
176 glass beads and 600 μL RLT buffer (Qiagen) with 10 $\mu\text{L mL}^{-1}$ β -mercaptoethanol
177 (Sigma, St Louis, USA). RNA samples were stored in liquid nitrogen or a deep freezer
178 at -80°C until analysis. Extraction and purification of RNA samples were performed
179 using the RNeasy extraction kit (Qiagen) on a vacuum manifold with on-column DNA
180 digestion using RNase-free DNase (Qiagen) according to the manufacturer's protocol.
181 RNA was eluted using 50 μL of RNase-free H_2O . Total RNA was then reverse
182 transcribed into complementary DNA (cDNA) using the PrimeScriptTM RT reagent Kit
183 with gDNA Eraser (TaKaRa) following the manufacturer's specifications.

184 Following Smith et al. (2006), we used double-stranded DNA and single-stranded
185 cDNA standards for DNA and cDNA quantification, respectively. Standard curves for
186 *rbcL* DNA were generated from plasmid DNA (pUC18, TaKaRa) containing an
187 artificial gene fragment (113 bp in size) of *rbcL* from the diatom *Thalassiosira*

188 *weissflogii* (CCMP1336). The plasmid DNA was linearized with *Hind*III (TaKaRa) and
189 quantified using a Thermo NanoDrop spectrophotometer (ND-1000). On the other hand,
190 to produce the cDNA standard, a PCR-amplified *rbcL* gene fragment of *T. weissflogii*
191 (CCMP1336) was inserted into a plasmid DNA (pCR2.1, Invitrogen). The plasmid
192 DNA was purified using the Plasmid maxi kit (Qiagen) and linearized with *Bam*HI
193 (TaKaRa), and in vitro transcription was performed using T7 RNA polymerase
194 (Invitrogen) for 2 hours at 37°C with Recombinant RNase Inhibitor (TaKaRa). To
195 eliminate DNA contamination, RNA was digested for 2 min at 42°C using gDNA
196 Eraser (TaKaRa). RNA was purified using an RNeasy column (Qiagen) following the
197 manufacturer's instructions and quantified with a Ribogreen RNA quantification kit
198 (Molecular Probes) using the manufacturer's standard. RNA was reverse transcribed
199 into cDNA using the PrimeScript™ RT reagent Kit with gDNA Eraser (TaKaRa).

200 Copy numbers of DNA and cDNA standards were calculated using the equation of
201 Smith et al. (2006), where the molecular mass of each nucleotide (or nucleotide pair) in
202 double- and single-stranded DNA is assumed to be 660 and 330 Da, respectively. Serial
203 dilutions of DNA and cDNA standards were prepared using sterilized Milli-Q water.

204 To amplify the *rbcL* gene and cDNA fragments from diatoms, the following specific
205 primer set designed by John et al. (2007a) was used.

206 Forward primer: 5'-GATGATGARAAYATTA ACTC-3'

207 Reverse primer: 5'-TAWGAACCTTTWACTTCWCC-3'.

208 Real-time PCR amplification was performed using SYBR Premix Ex Taq II (Perfect
209 Real Time, TaKaRa) with primer concentrations of 0.4 µM each and a Thermal Cycler
210 Dice Real Time System (TP800, TaKaRa). Diluted nucleic acid standards were then
211 added to the PCR mixture. The thermal cycling conditions were 95°C for 60 s, then 40
212 cycles of 95°C 5 s and 52°C 60 s. The fluorescence intensity of the complex formed by
213 SYBR green and the double-stranded PCR product was continuously monitored from
214 cycle 1 to 40. Quantification was achieved by the second-derivative maximum method
215 (Luu-The et al., 2005), and the copy number for each sample was determined by the
216 standard curves generated by serial dilutions of the standards.

217

218 **2.5 Clone libraries**

219 Clone libraries of *rbcL* cDNA were constructed for the C-380 and C-600 samples on
220 day 3, and Fe-380 and Fe-600 samples on day 2. The cDNA samples were PCR
221 amplified with the diatom-specific primer set and thermal cycling condition described
222 above using the TaKaRa Ex Taq Hot Start Version (TaKaRa). Triplicate PCR products
223 were mixed and then purified with agarose gel electrophoresis and the PureLink Quick
224 Gel Extraction Kit (Invitrogen). Purified amplicons from cDNA samples were then
225 cloned into the pCR2.1 vector using the TOPO TA cloning kit (Invitrogen) following
226 the manufacturer's instructions. Thirty-five to 50 colonies were randomly picked from
227 each clone library. Correct cDNA insertions were identified by PCR amplification using
228 the M13 forward (5'-GTAAAACGACGGCCAG-3') and reverse
229 (5'-CAGGAAACAGCTATGA-3') primers flanking the cloning site. Plasmid DNA
230 containing the inserts was cycle-sequenced using the Big Dye Terminator v3.1 Kit
231 (Applied Biosystems) with the M13 forward primer. The cycle sequencing products
232 were cleaned by isopropanol precipitation. Sequencing was performed with a 3130
233 Genetic Analyzer (Life Technologies). The obtained sequences were compared with
234 *rbcL* sequences deposited in GenBank database (<http://www.ncbi.nlm.nih.gov>) using
235 the BLAST query engine. Our *rbcL* cDNA sequences were deposited in the DDBJ
236 database with the following accession numbers: AB985799–AB986033.

237

238 **2.6 Phylogenetic and diversity analyses**

239 The *rbcL* sequences obtained were assembled into operational taxonomic units
240 (OTUs) with > 95% sequence identity, and rarefaction curves were plotted for each
241 clone library with the software mothur v. 1.27 (Schloss et al., 2009). To estimate OTU
242 richness, chao1 index (Chao, 1984) values were calculated using the number of
243 singleton sequences obtained in this study. Genetic diversity was assessed based on the
244 Shannon-Wiener index (H' , Shannon, 1948) and Simpson's index (D , Simpson, 1949).
245 The statistical significance of differences in the compositions of pairs of *rbcL* sequences
246 in the libraries was tested using LIBSHUFF (Singleton et al., 2001). The LIBSHUFF
247 program determined the integral form of the Cramer-von Mises statistic for each pair of
248 communities using 10,000 randomizations. Any two libraries were considered to be
249 significantly different from each other if the lower of the significance values generated

250 by the software was < 0.025 ($p < 0.05$).

251

252 **2.7 Statistical analysis**

253 Statistical analyses were performed with the program R (<http://www.r-project.org>).
254 To assess the statistically significant differences between $p\text{CO}_2$ levels in the control
255 treatments or between control and Fe treatments, Welch's t -test was used. Differences
256 among $p\text{CO}_2$ levels in the Fe-added treatments were evaluated with Kruskal-Wallis
257 one-way analysis of variance (ANOVA). Holm's test for multiple comparisons was
258 used to identify the source of the variance. For all of the analyses, the confidence level
259 was set at 95% ($p < 0.05$).

260

261 **3 Results**

262 **3.1 Experimental conditions**

263 The bubbling of CO_2 -controlled air succeeded in creating significant gradients in
264 $p\text{CO}_2$, pH, and DIC in the different CO_2 treatments except on day 4 in the Fe-added
265 treatments, when those values did not significantly differ between Fe-380 and Fe-600
266 (Table 1; Fig. S1). The initial concentrations of nitrate, phosphate, and silicic acid were
267 18.06 ± 0.10 , 1.47 ± 0.01 , and $16.90 \pm 0.12 \mu\text{mol L}^{-1}$, respectively (Table 1). In the
268 control bottles, these macronutrients remained until the end of the incubation in both
269 CO_2 treatments except for silicic acid, which was almost depleted on day 5 in the C-380
270 treatment (Fig. S2). In the Fe-added bottles, macronutrients were depleted on days 4 or
271 5 in all CO_2 treatments (Fig. S2). The TD-Fe concentration was 1.35 nmol L^{-1} in the
272 initial seawater, and it remained low throughout the experiment in the control treatments
273 (Table 1). In the Fe-added treatments, the TD-Fe concentrations were $5.50 \pm 0.10 \text{ nmol}$
274 L^{-1} in the initial bottles and remained above 4 nmol L^{-1} until the end of incubation
275 (Table 1). The initial Chl a concentration was $1.96 \pm 0.14 \mu\text{g L}^{-1}$ (Table 1). In the
276 control bottles, the Chl a concentration increased until the end of the incubation and
277 reached $10.22 \pm 0.89 \mu\text{g L}^{-1}$ in the C-380 and $6.28 \pm 0.64 \mu\text{g L}^{-1}$ in the C-600
278 treatments (Fig. S3). In the Fe-added bottles, the Chl a concentration increased rapidly
279 and reached the maximum on day 4 in the Fe-180 and Fe-380 treatments (27.51 ± 0.71
280 $\mu\text{g L}^{-1}$ and $28.45 \pm 3.40 \mu\text{g L}^{-1}$, respectively) and on day 5 in the Fe-600 and Fe-1000

281 treatments ($27.68 \pm 0.44 \mu\text{g L}^{-1}$ and $27.32 \pm 3.05 \mu\text{g L}^{-1}$, respectively), then declined
282 toward the end of the incubation (Fig. S3).

283

284 **3.2 Phytoplankton pigments**

285 Throughout the experiment, the concentrations of fucoxanthin (Fuco), mainly a
286 biomarker for diatoms (Ondrusek et al., 1991; Suzuki et al., 2011), and
287 19'-hexanoyloxyfucoxanthin (19'-Hex), an indicator of haptophytes (Jeffrey and Wright,
288 1994), were relatively high among the phytoplankton pigments. In the control bottles,
289 the concentrations of Fuco and 19'-Hex increased over time and reached the maximum
290 values on day 5 in both the C-380 and C-600 treatments (Figs. 1a and c). After day 3,
291 the concentrations of Fuco and 19'-Hex were higher in the C-380 treatment than in the
292 C-600 treatment (day 5: Welch's *t*-test C-380 > C-600, $p < 0.05$), although no statistical
293 significance was assessed on day 3 because samples were collected from each single
294 bottle. In the Fe-added bottles, Fuco concentrations increased throughout the incubation
295 and reached the maximum values on day 6, whereas 19'-Hex concentrations decreased
296 after day 4 (Figs. 1b and d). The concentrations of Fuco were significantly different
297 among CO₂ treatments on day 6 (Kruskal-Wallis ANOVA, $p < 0.05$), although these
298 differences were not supported by multiple comparisons (Holm's test, $p > 0.05$).
299 Significant differences among CO₂ treatments were also found for the 19'-Hex
300 concentration on day 6 (Kruskal-Wallis ANOVA, $p < 0.05$), and the values in the
301 Fe-180 treatment was significantly higher than those in the Fe-1000 treatment (Holm's
302 test, $p < 0.05$).

303

304 **3.3 CHEMTAX outputs**

305 In the initial phytoplankton community, diatoms and haptophytes were the
306 predominant numbers of the phytoplankton groups (i.e., they contributed 45% and 17%
307 of the Chl *a* concentration, respectively). The initial contributions of chlorophytes,
308 cryptophytes, peridinin-containing dinoflagellates, pelagophytes, prasinophytes, and
309 cyanobacteria to the Chl *a* biomass were 10%, 9%, 8%, 5%, 4%, and 2%, respectively.
310 In the control bottles, the contributions of diatoms to the Chl *a* biomass increased with
311 time, and their contributions reached the maximum (70% at the C-380 and 60% at the

312 C-600 treatments) on day 5 (Fig. 2a). On day 5, the contribution of diatoms in the
313 C-380 treatment was significantly higher than that in the C-600 treatment (Welch's
314 *t*-test, $p < 0.05$). However, the contribution of haptophytes to the Chl *a* biomass was
315 higher in the C-600 treatment (21%) than in the C-380 treatment (14%) on day 5
316 (Welch's *t*-test, $p < 0.05$). Increases in the contributions of diatoms were also observed
317 in the Fe-added treatment, and the contributions reached the maximum (82–85%) on
318 day 4 in all CO₂ treatments (Fig. 2b). In terms of diatom contribution, a significant
319 difference among CO₂ treatments was not detected with Kruskal-Wallis ANOVA ($p >$
320 0.05) in the Fe-added bottles. The contributions of haptophytes to Chl *a* biomass did not
321 differ significantly among CO₂ levels in the Fe-added bottles (Kruskal-Wallis ANOVA,
322 $p > 0.05$).

323

324 **3.4 Expression of diatom *rbcL* gene**

325 A significant linear relationship between the Fuco concentration and the
326 diatom-specific *rbcL* gene copy number was found (regression analysis: $r^2 = 0.677$, $p <$
327 0.001, $n = 28$) in our experiment (Fig. 3). In the control bottles, the transcript abundance
328 normalized to gene abundance (i.e., cDNA/DNA) of the diatom-specific *rbcL* gene
329 fragment for the C-380 treatment was significantly higher than that of the C-600
330 treatment on day 3 (Fig. 4; Welch's *t*-test, $p < 0.05$). In the Fe-added bottles, the
331 cDNA/DNA ratio of the diatom *rbcL* fragment in the lower CO₂ treatments (Fe-180 and
332 Fe-380) was higher than that in the Fe-600 treatment on day 2 (Fig. 4; Holm's test, $p <$
333 0.05).

334

335 **3.5 Clone libraries of diatom *rbcL* cDNA**

336 Rarefaction curves were plotted for the *rbcL* cDNA libraries (Fig. 5). In terms of
337 unique taxa, the highest number of OTUs was found in the C-380 treatment (Table 2).
338 The highest chao1 value was found in the C-600 treatment, whereas the lowest value
339 was found in the Fe-600 treatment. Shannon-Wiener and Simpson diversity indices
340 revealed that the cDNA libraries in the 380 ppm CO₂ bottles were more diverse than
341 those in the 600 ppm CO₂ bottles in both the control and Fe-added treatments, although
342 the values were not statistically significant between CO₂ treatments (*t*-test, $p > 0.05$)

343 (Table 2).

344 All sequences obtained from the cDNA libraries were more than 95% similar to
345 sequences deposited in the GenBank. These sequences could be classified into the
346 following 11 phylogenetic groups: Chaetocerotaceae, Coscinodiscaceae,
347 Cymatosiraceae, Stephanodiscaceae, Thalassiosiraceae, unidentified centrics,
348 Bacillariaceae, Naviculaceae, Fragillariaceae, unidentified pennates, and other
349 eukaryotes by comparison with known *rbcL* sequences from GenBank. Sequences that
350 could not be classified into a specific diatom family (e.g., closely related to two or more
351 diatom families with same similarity score) were assigned as unidentified centrics or
352 unidentified pennates. Other eukaryotes consisted of haptophytes, pelagophytes,
353 dictyochophytes, dinoflagellates, and diatoms which could **not** be assigned to centrics
354 and pennates. For all of the cDNA libraries, more than 88% of *rbcL* sequences were
355 most closely affiliated with those of cultured diatoms. In the initial cDNA library, the
356 most abundant sequences were closely affiliated with the diatom family Bacillariaceae
357 (46%), followed by other eukaryotes and Cymatosiraceae (17% and 14%, respectively)
358 (Fig. 6). The contributions of other diatom groups were less than 6% in the initial clone
359 library. In the control bottles, the contributions of Coscinodiscaceae increased to 12–
360 14%, whereas those of Cymatosiraceae decreased to 4%. In the Fe-added bottles, the
361 contributions of Chaetocerotaceae and unidentified centrics to the total increased to
362 more than 8% and 20%, respectively. In contrast, the contributions of Bacillariaceae
363 decreased below 24% in both the Fe-380 and Fe-600 treatments.

364 Statistic analysis using LIBSHUFF revealed that the cDNA libraries in the control
365 treatments were not significantly different from the initial sample regardless of the CO₂
366 level, whereas those in the Fe-added bottles differed significantly from the initial
367 assemblage (LIBSHUFF, $p < 0.05$) (Table 3). No significant difference in the cDNA
368 library was found between C-380 and C-600 treatments in the control bottles
369 (LIBSHUFF, $p > 0.05$). However, a significant difference between the Fe-380 and
370 Fe-600 treatments was detected in the Fe-added bottles (LIBSHUFF, $p < 0.05$). In
371 addition, cDNA libraries in the Fe-added bottles differed significantly from those of the
372 control bottles in both the Fe-380 and Fe-600 treatments (LIBSHUFF, $p < 0.05$).

373

374 4 Discussion

375 4.1 Changes in phytoplankton community structure during incubation

376 Our CHEMTAX analysis suggested that the diatoms were the principal contributors
377 to the Chl *a* biomass in the initial phytoplankton community, followed by haptophytes
378 (Fig. 2). The results were consistent with those reported by Suzuki et al. (2002), who
379 examined the community structure in the Bering Sea during early summer of 1999.
380 These results suggest that diatoms and haptophytes are ecologically important
381 phytoplankton groups in the study area during the summer. Compared with previous
382 reports in the area (Suzuki et al., 2002; Yoshimura et al., 2013), a relatively high initial
383 Chl *a* concentration was observed in our experiment, possibly due to an intrusion of the
384 coastal seawater mass from the Aleutian trenches (Sugie et al., 2013). However, the Fe
385 infusion induced significant increases in Chl *a* biomass and concomitant rapid
386 drawdowns of macronutrients in our incubation bottles (Fig. S2). This indicates that the
387 seawater used for the incubation was Fe-limited for phytoplankton assemblages. Our
388 HPLC and CHEMTAX results suggested that the increase in phytoplankton biomass
389 was mainly due to an increase in diatoms (Figs. 1b and 2b).

390 We found that the growth of Fuco was less in the high CO₂ bottles in the control
391 treatments (Fig. 1a), suggesting that the elevated CO₂ levels could have a negative
392 impact on the diatom biomass in the study area. Negative effects on diatoms induced by
393 an increase in CO₂ availability were also reported in field incubation experiments
394 conducted in the Bering Sea and the Okhotsk Sea (Hare et al., 2007 and Yoshimura et
395 al., 2010, respectively). However, such trends have rarely been observed in other
396 regions of the world's oceans (e.g., Tortell et al., 2002; Kim et al., 2006; Feng et al.,
397 2009; Hoppe et al., 2013; Endo et al., 2013). Therefore, the responses of phytoplankton
398 assemblages to ocean acidification can differ among geographic locations due to the
399 differences in the biogeography of phytoplankton and/or environmental conditions.

400 One possible cause of the geographic specificity in the open Bering Sea is the
401 differences in the species composition of diatoms. Our microscope data showed that
402 centric diatoms such as Chaetocerataceae and Rhizosoleniaceae were predominant at
403 the beginning of the incubation in terms of carbon biomass, and the coastal diatom
404 species *Chaetoceros* spp. became predominant in all incubation bottles after day 2
405 (Sugie et al., 2013). Therefore, the relative decrease in Fuco biomass with increased

406 CO₂ levels might be partially explained by the decrease in *Chaetoceros* spp. A previous
407 field incubation experiment conducted in the Bering Sea also showed that the carbon
408 biomass of the *Chaetoceros* spp. decreased at higher CO₂ levels (600–960 μatm CO₂),
409 although it increased at 1190 μatm CO₂ (Yoshimura et al., 2013). However, Tortell et al.
410 (2008) demonstrated that relative abundance of *Chaetoceros* spp. increased under
411 elevated CO₂ levels in the Ross Sea. In the previous laboratory culture experiments, the
412 effects of increased CO₂ on the growth and/or photosynthesis of *Chaetoceros* spp. were
413 also inconsistent. For example, Ihnken et al. (2011) demonstrated that the growth of
414 diatom *Chaetoceros muelleri* decreased with elevated CO₂ (decreased pH) levels
415 although their photosynthetic capacity increased. In contrast, Trimborn et al. (2013)
416 showed a significant increase in the growth rate of *Chaetoceros debilis* under high CO₂
417 condition. In addition, no CO₂-related change in the growth and photosynthetic
418 physiology of *Chaetoceros brevis* was found (Boelen et al., 2011). These results suggest
419 that the responses to elevated CO₂ differ among *Chaetoceros* species.

420 The concentrations of 19'-Hex were significantly lower in the C-600 treatment than
421 those in the C-380 treatment (Fig. 1c), suggesting that the ocean acidification could
422 induce negative effects not only on the biomass of diatoms, but also on that of
423 haptophytes in the study area. Similar results were obtained from the previous field
424 studies in other regions (e.g., Feng et al., 2010; Endo et al., 2013). One possible factor
425 underlying these decreases is that the reduced carbonate-saturation states under high
426 CO₂ conditions. The energetic cost of calcification in coccolithophores will increase
427 with a decrease in pH (Mackinder et al., 2010). Therefore, additional energy might be
428 needed for cell growth in seawater with high CO₂ levels. In addition, non-calcifying
429 haptophytes such as *Phaeocystis* spp. often dominate among haptophytes in the natural
430 phytoplankton community (Schoemann et al., 2005), although the effects of ocean
431 acidification on them are still not well understood. Therefore, additional study using a
432 wide range of haptophyte species would be required for a detailed understanding of the
433 responses of the haptophyte community to CO₂-induced ocean acidification.

434 Our CHEMTAX outputs showed that the relative contributions of diatoms decreased
435 with increased CO₂ levels, whereas the contributions of haptophytes increased in both
436 the control and Fe-added bottles (Fig. 2). This indicates that the negative impacts of
437 increased CO₂ on diatoms were greater than those on haptophytes and other

438 phytoplankton groups. Another possibility is that the competitions between diatoms and
439 other phytoplankton taxa could occur. For example, diatoms could become less
440 competitive when silicic acid is exhausted, because Si-depletion significantly depressed
441 the growth and could induce their cell death (Harrison et al., 1977; Jiang et al. 2014).
442 However, concentrations of silicic acid were not significantly different among CO₂
443 levels in the Fe-added treatments (Fig. S2f). Moreover, in the control treatments, silicic
444 acid was almost depleted in the low CO₂ treatment after day 5 but not in the high CO₂
445 treatment (Fig. S2e). These results suggest that availability of silicic acid little affected
446 the decreases in relative diatom contribution to Chl *a* biomass. Larger diatoms can
447 contribute to efficient transfer of energy and organic compounds to higher trophic levels
448 because they would create a shorter food chain compared with nano- and pico-sized
449 phytoplankton (Michaels and Silver, 1988). Because diatoms form a large part of
450 phytoplankton biomass in the Bering Sea basin (Suzuki et al., 2002; Takahashi et al.,
451 2002), the decrease in the relative contribution of diatoms with increasing CO₂ could
452 reduce the energy transferred from the primary producers to the higher trophic levels.

453 The decreases in Fuco growth and relative contribution of diatoms were larger in the
454 control bottles than those in the Fe-added treatments (Figs. 1 and 2), suggesting that the
455 negative effect of CO₂ enrichment was greater in the Fe-limited conditions. These
456 results are consistent with Sugie et al. (2013) and Yoshimura et al. (2014), who
457 observed significant decreases in diatom carbon biomass and particulate organic carbon
458 (POC) production under high CO₂ levels in the control treatments, whereas those were
459 insignificantly changed in the Fe-added treatments. Sugie et al. (2013) indicated that the
460 Fe limitations for phytoplankton in the control bottles were enhanced at high CO₂ levels,
461 likely due to the reduction of Fe bioavailability as reported in Shi et al. (2010). The
462 combined effects of CO₂ and Fe availability were also tested in a diatom-dominated
463 phytoplankton community in the Southern Ocean (Hoppe et al., 2013). In their study,
464 net primary productivity in seawater decreased with increased *p*CO₂ levels in the
465 Fe-depleted treatments but not in the Fe-enriched treatments. These studies indicate that
466 an interactive effect of CO₂ enrichment and Fe limitation could occur in the
467 diatom-dominated natural phytoplankton assemblages in the HNLC region.

468

469 **4.2 *rbcL* expression in diatoms**

470 A significant correlation between diatom *rbcL* copies per liter and Fuco
471 concentration was found in this study (Fig. 3), suggesting the usefulness of the *rbcL*
472 gene fragment as a proxy for diatoms. In addition, the cDNA sequences obtained from
473 cloning were dominated by the diatom-derived *rbcL* gene (Fig. 6). These results
474 indicate that the *rbcL* primers used successfully and selectively amplified the *rbcL* gene
475 of diatoms. Suzuki et al. (2011) showed that Fuco concentration significantly correlated
476 with diatom carbon biomass in the subarctic Pacific. Furthermore, Matsuda et al. (2011)
477 showed that the number of *rbcL* gene per cell varies among diatom species, and it was
478 positively correlated with cell size. Therefore, we concluded that the *rbcL* gene could
479 serve as a potential molecular marker for diatom biomass.

480 The **transcript abundance** of the diatom-specific *rbcL* gene decreased with elevated
481 CO₂ levels in both the control and Fe-added treatments (Fig. 4). Because RubisCO
482 expression is primarily controlled at the transcriptional level in the natural
483 phytoplankton community (Xu and Tabita, 1996; Wawrik et al., 2002), our results
484 suggest that increased CO₂ levels could reduce the amount of RubisCO in diatoms. It
485 should be noted that significant decreases in *rbcL* expression with increased CO₂ levels
486 were observed on days 2 or 3, when macronutrients still remained (Fig. S2). This
487 indicates that the downregulation of *rbcL* expression in diatoms was probably caused by
488 the increase in CO₂ availability. It has been shown that some land plants can increase
489 their nitrogen utilization efficiency under elevated CO₂ levels by reducing the
490 investment of nitrogen in RubisCO (Curtis et al., 1989; Makino et al., 2003). Losh et al.
491 (2012; 2013) also demonstrated a decreased RubisCO contribution to the total protein in
492 the California Current phytoplankton community with an increase in CO₂ level.
493 Because a decrease in the expression of RubisCO can result in a reduction of the
494 potential capacity for carbon fixation in the natural environment (John et al., 2007b),
495 our results indicate that an increase in CO₂ levels could have a negative impact on
496 photosynthetic carbon fixation for diatoms in the study area. Recently, Gontero and
497 Salvucci (2014) pointed out that RubisCO activase plays a key role in the modification
498 of RubisCO activity, and consequently in the capacity of carbon fixation, although the
499 occurrence of RubisCO activase in diatoms is not well understood. Further studies must
500 be needed for better understanding of the impacts of elevated CO₂ on photosynthetic

501 physiology in diatoms.

502 The negative effects of increasing CO₂ on diatom biomass were not severe in the
503 Fe-added bottles relative to Fe-limited control bottles (Figs. 1a and b), whereas *rbcL*
504 transcripts decreased with increased CO₂ regardless of Fe availability (Fig. 4). This
505 suggests that the diatoms could overcome the decrease in RubisCO activity in the
506 Fe-added treatments. According to our cloning data (Fig. 6), a shift in phylogenetic
507 composition of the diatoms actively transcribed *rbcL* was observed in the Fe-added
508 bottles. In addition, F_v/F_m values increased significantly with Fe enrichment in our
509 incubation experiments (Sugie et al., 2013), indicating an increase in the photochemical
510 quantum efficiency of photosystem II for the diatoms. Therefore, the photosystem II
511 activity might compensate for the decrease in RubisCO expression under Fe-replete
512 conditions.

513 It is generally recognized that phytoplankton autonomously regulate the transcription
514 of the *rbcL* gene in response to environmental conditions such as light and nutrient
515 availability (Pichard et al., 1996; Granum et al., 2009; John et al., 2010). However, the
516 mechanisms controlling the transcription of RubisCO operon in diatoms are largely
517 unknown. Recently, Minoda et al. (2010) showed that the red alga *Cyanidioschyzon*
518 *merolae* increased *rbcL* transcription at high levels of NADPH, 3-phosphoglyceric acid
519 (3-PGA), or ribulose-1,5-bisphosphate (RuBP) under the influence of the transcription
520 factor Ycf30. In addition, it has been reported that regeneration of RuBP could be a
521 limiting factor for the CBB cycle in high CO₂ conditions (von Caemmerer and Farquhar,
522 1981; Stitt, 1991; Onoda et al., 2005). Thus, one possible mechanism underlying the
523 reduction of diatom *rbcL* transcripts observed in our study is related to a decrease in
524 RuBP concentration in the chloroplasts due to the increase in CO₂ availability for
525 diatoms. Because diatoms possess the same type of RubisCO (Form ID) and gene
526 homologs encoding the Ycf30 protein (i.e., *ycf30*) (Kowallik et al., 1995), they could
527 control *rbcL* gene expression using the same mechanisms as *C. merolae*. Further studies
528 using marine diatom cultures are required to obtain a better understanding of the
529 physiological mechanisms controlling the expression of RubisCO.

530 In our experiment, the rarefaction curves plateaued to some extent in all treatments
531 (Fig. 5), indicating that the clone numbers screened from each library were statistically

532 sufficient for further diversity analysis. Taxonomic compositions in the cDNA library
533 were considerably different from those in the diatom carbon biomass revealed by
534 microscopic analysis by Sugie et al. (2013), which were composed primarily by
535 Chaetocerataceae. This implies that the predominant diatoms did not necessarily
536 become transcriptionally active *rbcL* phylotypes in our experiment. In addition, because
537 16–42% of the sequences were classified as unidentified diatoms or other eukaryotes,
538 the primer set used in this study might be insufficient to estimate diatom composition at
539 the family level.

540 The *rbcL* cDNA libraries in the Fe-added treatments differed significantly from the
541 initial library, whereas those in the control treatments were not significantly different
542 (Table 3), suggesting that the diatom blooms induced by Fe infusion were associated
543 with the change in the relative contribution of *rbcL* expression in diatoms. For example,
544 compared to the initial seawater, the relative contributions of Chaetocerataceae and
545 unidentified centrics to the *rbcL* cDNA library increased markedly in the Fe-added
546 bottles whereas they remained minor components in the control bottles (Fig. 6). This
547 indicates that the relative significance of the RubisCO activity of these phylotypes could
548 be increased by Fe enrichment. In addition, cDNA libraries were significantly different
549 from each other at different CO₂ levels in the Fe-added bottles (Table 3). This indicates
550 that the transcriptionally active phylotypes in diatoms could shift in response to an
551 increase in the CO₂ level. On the other hand, the diversity indices for the
552 diatom-specific *rbcL* cDNA sequences were not affected by CO₂ availability (Table 2).
553 In addition, the highest chao1 (richness) value was observed in C-600 treatment. These
554 results suggest that the richness and/or diversity of diatom phylotypes actively
555 transcribing *rbcL* gene could remain under elevated CO₂ levels.

556

557 **5 Conclusions**

558 The present study showed that an increase in CO₂ levels could have negative impacts
559 on diatom biomass in the Bering Sea, especially under Fe-limited conditions. Because
560 diatoms play pivotal roles in carbon sequestration and food webs in the Bering Sea
561 (Springer et al., 1996; Takahashi et al., 2002), our results indicate that ocean
562 acidification might alter the biogeochemical processes and ecological dynamics in the

563 study area. Although the present results cannot be extrapolated to other HNLC
564 ecosystems due to differences in other environmental conditions, our findings suggest
565 that the combined effects of CO₂ and other environmental factors such as Fe availability
566 need to be examined for a better understanding of the potential impacts of ocean
567 acidification on marine ecosystems.

568 We examined, for the first time, the relationships between CO₂ levels or Fe
569 availability and RubisCO expression of diatoms in the Bering Sea. Significant decreases
570 in the *rbcL* expression of diatoms were observed at elevated CO₂ levels in both the
571 Fe-limited and Fe-enriched treatments, suggesting that ocean acidification could reduce
572 the primary productivity in the study area. Our results indicate that the amount of *rbcL*
573 transcripts could be an important indicator to assess the physiological responses of
574 RubisCO activity in diatoms to environmental drivers. However, photosynthetic carbon
575 fixation in diatoms can be controlled not only by RubisCO activity, but also other
576 processes such as carbon concentrating mechanisms (CCMs) and/or RuBP regeneration
577 (Rost et al., 2003; Onoda et al., 2005). More detailed studies on molecular mechanisms
578 are required to clarify the physiological responses of the diatom community to CO₂ and
579 Fe availability.

580

581 **6 Acknowledgements**

582 We thank the captain, officers, and crew of the R/V *Hakuho Maru* for their great
583 support and field assistance. We also thank J. Nishioka for Fe analysis. We also
584 appreciate the editor and three referees for providing constructive comments on the
585 manuscripts. This work was conducted within the framework of the Plankton
586 Ecosystem Response to CO₂ Manipulation Study (PERCOM) and was partly supported
587 by the grants from CRIEPI (#090313) and Grant-in-Aid for Scientific Research
588 (#18067008, #22681004).

589

590 **7 References**

591 Badger, M. R., Whitney, S. M., Ludwig, M., Yellowlees, D. C., Leggat, W., and Price,
592 G. D.: The diversity and co-evolution of RubisCO, plastids, pyrenoids, and
593 chloroplast based CO₂-concentrating mechanisms in algae, *Can. J. Bot.*, 76, 1052–

- 594 1071, 1998.
- 595 Banse, K., and English, D. C.: Comparing phytoplankton seasonality in the eastern and
596 western subarctic Pacific and the western Bering Sea, *Prog. Oceanogr.*, 43, 235–
597 288, 1999.
- 598 Boelen, P., van de Poll, W. H., van de Strate, H. J., Neven, I. A., Beardall, J., Buma, A.
599 G. J.: Neither elevated nor reduced CO₂ affects the photophysiological
600 performance of the marine Antarctic diatom *Chaetoceros brevis*, *J. Exp. Mar. Biol.*
601 *Ecol.*, 406, 38–45, 2011.
- 602 Caldeira, K., and Wickett, M. E.: Anthropogenic carbon and ocean pH. *Nature*, 425,
603 365, 2003.
- 604 Chao, A.: Nonparametric estimation of the number of classes in a population. *Scand. J.*
605 *Stat.*, 265–270, 1984.
- 606 Collins, S., Rost, B., and Rynearson, T. A.: Evolutionary potential of marine
607 phytoplankton under ocean acidification, *Evol. Appl.*, 7, 140–155, 2014.
- 608 Corredor, J. E., Wawrik, B., Paul, J. H., Tran, H., Kerkhof, L., Lopez, J. M., Dieppa, A.,
609 and Cardenas, O.: Geochemical rate-RNA integrated study:
610 ribulose-1,5-bisphosphate carboxylase/oxygenase gene transcription and
611 photosynthetic capacity of planktonic photoautotrophs, *Appl. Environ. Microbiol.*,
612 70, 5459–5468, 2004.
- 613 Curtis, P. S., Drake, B. G., and Whigham, D. F.: Nitrogen and carbon dynamics in C₃
614 and C₄ marsh plants grown under elevated CO₂ in situ, *Oecologia*, 78, 297–301,
615 1989.
- 616 Edmond, J. M.: High precision determination of titration alkalinity and total carbon
617 dioxide content of sea water by potentiometric titration, *Deep-Sea Res.*, 17, 737–
618 750, 1970.
- 619 Endo, H., Yoshimura, T., Kataoka, T., and Suzuki, K.: Effects of CO₂ and iron
620 availability on phytoplankton and eubacterial community compositions in the
621 northwest subarctic Pacific, *J. Exp. Mar. Biol. Ecol.*, 439, 160–175, 2013.
- 622 Engel, A., Schulz, K. G., Riebesell, U., Bellerby, R., Delille, B., Schartau, M.: Effects
623 of CO₂ on particle size distribution and phytoplankton abundance during a
624 mesocosm bloom experiment (PeECE II), *Biogeosciences*, 5, 509–521, 2008.
- 625 Feng, Y., Hare, C. E., Leblanc, K., Rose, J. M., Zhang, Y., DiTullio, G. R., Lee, P. A.,
626 Wilhelm, S. W., Rowe, J. M., Sun, J., Nemcek, N., Gueguen, C., Passow, U.,
627 Benner, I., Brown, C., and Hutchins, D. A.: Effects of increased pCO₂ and
628 temperature on the North Atlantic spring bloom. I. The phytoplankton community
629 and biogeochemical response, *Mar. Ecol. Prog. Ser.* 388, 13–25, 2009.
- 630 Feng, Y., Hare, C. E., Rose, J. M., Handy, S. M., DiTullio, G. R., Lee, P. A., Smith Jr,
631 W. O., Peloquin, J., Tozzi, S., Sun, J., Zhang, Y., Dunbar, R. B., Long, M. C.,
632 Sohst, B., Lohan, M., and Hutchins, D. A.: Interactive effects of iron, irradiance

- 633 and CO₂ on Ross Sea phytoplankton, *Deep-Sea Res. I*, 57, 368–383, 2010.
- 634 Gontero, B., and Salvucci, M. E.: Regulation of photosynthetic carbon metabolism in
635 aquatic and terrestrial organisms by Rubisco activase, redox-modulation and
636 CP12, *Aquat. Bot.*, 118, 14–23, 2014.
- 637 Granum, E., Roberts, K., Raven, J. A., Leegood, R. C.: Primary carbon and nitrogen
638 metabolic gene expression in the diatom *Thalassiosira pseudonana*
639 (Bacillariophyceae): Diel periodicity and effects of inorganic carbon and nitrogen,
640 *J. Phycol.*, 45, 1083–1092, 2009.
- 641 Hare, C. E., Leblanc, K., DiTullio, G. R., Kudela, R. M., Zhang, Y., Lee, P. A.,
642 Riseman, S., and Hutchins, D. A.: Consequences of increased temperature and
643 CO₂ for phytoplankton community structure in the Bering Sea, *Mar. Ecol. Prog.*
644 *Ser.*, 352, 9–16, 2007.
- 645 Harrison, P.J., Conway, H.L., Holmes, R.W., and Davis, C.O.: Marine diatoms grown
646 in chemostats under silicate or ammonium limitation. III. Cellular chemical
647 composition and morphology of *Chaetoceros debilis*, *Skeletonema costatum*, and
648 *Thalassiosira gravida*, *Mar. Biol.*, 43(1), 19–31, 1977.
- 649 Hoppe, C. J., Hassler, C. S., Payne, C. D., Tortell, P. D., Rost, B. and Trimborn, S.: Iron
650 limitation modulates ocean acidification effects on Southern Ocean phytoplankton
651 communities, *PloS One*, 8(11), e79890, 2013.
- 652 Ihnken, S., Roberts, S., and Beardall, J.: Differential responses of growth and
653 photosynthesis in the marine diatom *Chaetoceros muelleri* to CO₂ and light
654 availability, *Phycologia*, 50, 182–193, 2011.
- 655 Jeffrey, S.W., and Wright, S.W.: Photosynthetic pigments in the Haptophyta, in: *The*
656 *Haptophyte algae*, Green, J. C., and Leadbeater, B. S. C. (Eds.), Carendon Press,
657 Oxford, 111–132, 1994.
- 658 Jiang, Y., Yin, K., Berges, J.A., and Harrison, P.J.: Effects of silicate resupply to
659 silicate-deprived *Thalassiosira weissflogii* (Bacillariophyceae) in stationary or
660 senescent phase: short-term patterns of growth and cell death, *J. Phycol.*, 50(3),
661 602–606, 2014
- 662 John, D. E., Jose, López-Díaz, J. M., Cabrera, A., Santiago, N. A., Corredor, J. E.,
663 Bronk, D. A., and Paul, J. H.: A day in the life in the dynamic marine
664 environment: how nutrients shape diel patterns of phytoplankton photosynthesis
665 and carbon fixation gene expression in the Mississippi and Orinoco River plumes,
666 *Hydrobiologia*, 679, 155–173, 2010.
- 667 John, D. E., Patterson, S. S., and Paul, J. H.: Phytoplankton group specific quantitative
668 polymerase chain reaction assays for RuBisCO mRNA transcripts in seawater,
669 *Mar. Biotechnol.*, 9, 747–759, 2007a.
- 670 John, D. E., Wang, Z. A., Liu, X. W., Byrne, R. H., Corredor, J. E., Lopez, J. M.,
671 Cabrera, A., Bronk, D. A., Tabita, F. R., and Paul, J. H.: Phytoplankton carbon
672 fixation gene (RuBisCO) transcripts and air-sea CO₂ flux in the Mississippi River

- 673 plume, *ISME J.*, 1, 517–531, 2007b.
- 674 Kim, J. -M., Lee, K., Shin, K., Kang, J. -H., Lee, H. -W., Kim, M., Jang, P. -G., and
675 Jang, M. -C.: The effect of seawater CO₂ concentration on growth of the natural
676 phytoplankton assemblage in a controlled mesocosm experiment, *Limnol.*
677 *Oceanogr.*, 51, 1629–1636, 2006.
- 678 Kowallik, K. V., Stoebe, B., Schaffran, I., KrothPancic, P., and Freier, U.: The
679 chloroplast genome of a chlorophyll *a+c*-containing alga, *Odontella sinensis*,
680 *Plant Mol. Biol. Rep.*, 13, 336–342, 1995.
- 681 Latasa, M.: Improving estimations of phytoplankton class abundances using
682 CHEMTAX, *Mar. Ecol. Progr. Ser.*, 329, 13–21, 2007.
- 683 Lewis, E., and Wallance, D. W. R.: Program developed for CO₂ system calculations.
684 ORNL/CDIAC-105. Carbon dioxide information analysis center, Oak Ridge
685 National Laboratory, US Department of Energy, Oak Ridge, Tennessee, 1998.
- 686 Losh, J. L., Morel, F. M. M., and Hopkinson, B. M.: Modest increase in the C:N ratio of
687 N-limited phytoplankton in the California Current in response to high CO₂, *Mar.*
688 *Ecol. Prog. Ser.*, 468, 31–42, 2012.
- 689 Losh, J. L., Young, J. N., and Morel, F. M.: Rubisco is a small fraction of total protein
690 in marine phytoplankton, *New Phytol.*, 198, 52–58, 2013.
- 691 Luu-The, V., Paquet, N., Calvo, E., and Cumps, J.: Improved real-time RT-PCR method
692 for high-throughput measurements using second derivative calculation and double
693 correction, *Biotechniques*, 38, 287–293, 2005.
- 694 Mackey, M. D., Mackey, D. J., Higgins, H. W., and Wright, S. W.: CHEMTAX-a
695 program for estimating class abundances from chemical markers: application to
696 HPLC measurements of phytoplankton, *Mar. Ecol. Progr. Ser.*, 144, 265–283,
697 1996.
- 698 Mackinder, L., Wheeler, G., Schroeder, D., Riebesell, U., and Brownlee, C.: Molecular
699 mechanisms underlying calcification in coccolithophores, *Geomicrobiology*, 27,
700 585–595, 2010.
- 701 Makino, A., Sakuma, H., Sudo, E., and Mae, T.: Differences between Maize and Rice in
702 N-use efficiency for photosynthesis and protein allocation, *Plant Cell Physiol.*, 44,
703 952–956, 2003.
- 704 Matsuda, Y., Nakajima, K., and Tachibana, M.: Recent progresses on the genetic basis
705 of the regulation of CO₂ acquisition systems in response to CO₂ concentration,
706 *Photosynth. Res.*, 109, 191–203, 2011.
- 707 Meakin, N. G., and Wyman, M.: Rapid shifts in picoeukaryote community structure in
708 response to ocean acidification, *ISME J.*, 5, 1397–1405, 2011.
- 709 Meehl, G. A., Stocker, T. F., Collins, W. D., Friedlingsten, P., Gaye, A. T., Gregory, J.
710 M., Kitoh, A., Knutti, R., Murphy, J. M., Noda, A., Raper, S. C. B., Watterson, I.

- 711 G., Weaver, A. J., and Zhao, Z. -C.: Global Climate Projections, in: Climate
712 Change 2007 The Physical Science Basis, Contribution of Working Group I to the
713 Fourth Assessment Report of the Intergovernmental Panel on Climate Change,
714 Solomon, S., Qin, D., Manning, M., Chen, Z., Marquis, M., Averyt, K., Tignor, M.
715 M. B., and Miller, H.L (EDs.), Cambridge University Press, United Kingdom and
716 New York, 2007.
- 717 Michaels, A. F., and Silver, M. W.: Primary Production, sinking fluxes and the
718 microbial food web, *Deep-Sea Res.* 35, 473–490, 1988.
- 719 Minoda, A., Weber, A. P. M., Tanaka, K., and Miyagishima, S.: Nucleus-independent
720 control of the Rubisco operon by the plastid-encoded transcription factor Ycf30 in
721 the red alga *Cyanidioschyzon merolae*, *Plant Physiol.*, 154, 1532–1540, 2010.
- 722 Obata, H., Karatani, H., and Nakayama, E.: Automated determination of iron in
723 seawater by chelating resin concentration and chemiluminescence detection, *Anal.*
724 *Chem.*, 65, 1524–1528, 1993.
- 725 Ondrusek, M. E., Bidigare, R. R., Sweet, S. T, Defreitas, D. A., and Brooks, J. M.:
726 Distribution of phytoplankton pigments in the North Pacific Ocean in relation to
727 physical and optical variability, *Deep-Sea Res.*, 38, 243-266, 1991.
- 728 Onoda, Y., Hikosaka, K., and Hirose, T.: Seasonal change in the balance between
729 capacities of RuBP carboxylation and RuBP regeneration affects CO₂ response of
730 photosynthesis in *Polygonum cuspidatum*, *J. Exp. Bot.*, 56, 755–763, 2005.
- 731 Pearson, P. N., and Palmer, M. R.: Atmospheric carbon dioxide concentration over the
732 past 60 million years, *Nature*, 406, 659–699, 2000.
- 733 Pichard, S. L., Campbell, L., Kang, J. B., Tabita, F. R., and Paul, J. H.: Regulation of
734 ribulose biphosphate carboxylase gene expression in natural phytoplankton
735 communities 1. Diel rhythms, *Mar. Ecol. Progr. Ser.*, 139, 257–265, 1996.
- 736 Raven, J., Caldeira, K., Elderfield, H., Hoegh-Guldberg, O., Liss, P., Riebesell, U.,
737 Shepherd, J., Turley, C., and Watson, A.: Ocean acidification due to increasing
738 atmospheric carbon dioxide, The Royal Society policy document 12/05, Cardiff:
739 Clyvedon Press, 2005.
- 740 Riebesell, U., Schulz, K. G., Bellerby, R. G. J., Botros, M., Fritsche, P., Meyerhöfer, M.,
741 Neill, C., Nondal, G., Oschlies, A., Wohlers, J., and Zöllner, E.: Enhanced
742 biological carbon consumption in a high CO₂ ocean, *Nature*, 450 (7169), 545–548,
743 2007.
- 744 Riebesell, U., and Tortell, P. D.: Effects of ocean acidification on pelagic organisms and
745 ecosystems, in: *Ocean acidification*, Gattuso, J.-P., and Hansson, L. (Eds.),
746 Oxford University Press, New York, 83–98, 2011.
- 747 Rost, B., Riebesell, U., Burkhardt, S., and Sültemeyer, D.: Carbon acquisition of bloom
748 forming marine phytoplankton, *Limnol. Oceanogr.* 48, 55–67, 2003.

- 749 Sabine, C. L., Feely, R. A., Gruber, N., Key, R. M., Lee, K., Bullister, J.L., Wanninkhof,
750 R., Wong, C. S., Wallace, D. W. R., Tilbrook, B., Millero, F. J., Peng, T. -H.,
751 Kozyr, A., Ono, T., and Rios, A. F.: The oceanic sink for anthropogenic CO₂,
752 Science, 305, 367–371, 2004.
- 753 Schloss, P. D., Westcott, S. L., Ryabin, T., Hall, J. R., Hartmann, M., Hollister, E. B.,
754 Lesniewski, R. A., Oakley, B. B., Parks, D. H., Robinson, C. J., Sahl, J. W., Stres,
755 B., Thallinger, G. G., Van Horn, D. J., and Weber, C. F.: Introducing mothur:
756 open-source, platform-independent, community-supported software for describing
757 and comparing microbial communities, Appl. Environ. Microbiol., 75, 7537–7541,
758 2009.
- 759 Schoemann, V., Becquevort, S., Stefels, J., Rousseau, V., and Lancelot, C.: Phaeocystis
760 blooms in the global ocean and their controlling mechanisms: a review, J. Sea
761 Res., 53, 43–66, 2005.
- 762 Shannon, C. E.: A mathematical theory of communication, AT&T Teck. J., 27, 379–423,
763 1948.
- 764 Shi, D., Xu, Y., Hopkinson, B. M., Morel, F. M. M.: Effect of ocean acidification on
765 iron availability to marine phytoplankton, Science, 327, 676–679, 2010.
- 766 Simpson, E. H.: Measurement of diversity, Nature, 163, 688, 1949.
- 767 Singleton, D. R., Furlong, M. A., Rathbun, S. L., and Whitman, W. B.: Quantitative
768 comparisons of 16S rRNA gene sequence libraries from environmental samples,
769 Appl. Environ. Microbiol., 67, 4374–4376, 2001.
- 770 Smith, C. J., Nedwell, D. B., Dong, L. F., and Osborn, A. M.: Evaluation of quantitative
771 polymerase chain reaction-based approaches for determining gene copy and gene
772 transcript number in environmental samples, Environ. Microbiol., 8, 804–815,
773 2006.
- 774 Springer, A. M., McRoy, C. P., and Flint, M. V.: The Bering Sea Green Belt: shelf-edge
775 processes and ecosystem production, Fish. Oceanogr., 5, 205–223, 1996.
- 776 Stitt, M.: Rising CO₂ levels and their potential significance for carbon flow in
777 photosynthetic cells, Plant Cell Environ., 14, 741–762, 1991.
- 778 Sugie, K., Endo, H., Suzuki, K., Nishioka, J., Kiyosawa, H., and Yoshimura, T.:
779 Synergistic effects of *p*CO₂ and iron availability on nutrient consumption ratio of
780 the Bering Sea phytoplankton community, Biogeosciences, 10, 6309–6321, 2013.
- 781 Suzuki, K., Kuwata, A., Yoshie, N., Shibata, A., Kawanobe, K., and Saito, H.:
782 Population dynamics of phytoplankton, heterotrophic bacteria, and viruses during
783 the spring bloom in the western subarctic Pacific, Deep-Sea Res. I, 58, 575–589,
784 2011.
- 785 Suzuki, K., Minami, C., Liu, H., and Saino, T.: Temporal and spatial patterns of
786 chemotaxonomic algal pigments in the subarctic Pacific and the Bering Sea
787 during the early summer of 1999, Deep-Sea Res. II, 49, 5685–5704, 2002.

- 788 Takahashi, K., Fujitani, N., and Yanada, M.: Long term monitoring of particle fluxes in
789 the Bering Sea and the central subarctic Pacific Ocean, 1990–2000, *Prog.*
790 *Oceanogr.*, 55, 95–112, 2002.
- 791 Tortell, P. D., DiTullio, G. R., Sigman, D. M., and Morel, F. M. M.: CO₂ effects on
792 taxonomic composition and nutrient utilization in an Equatorial Pacific
793 Phytoplankton assemblage, *Mar. Ecol. Prog. Ser.*, 236, 37–43, 2002.
- 794 Tortell, P. D., Payne, C. D., Li, Y., Trimborn, S., Rost, B., Smith, W. O., Riesselan, C.,
795 Dunbar, R. B., Sedwick, P., and DiTullio, G. R.: CO₂ sensitivity of Southern
796 Ocean phytoplankton, *Geophys. Res. Lett.*, 35(4), L04605, 2008.
- 797 Trimborn, S., Brenneis, T., Sweet, E., and Rost, B.: Sensitivity of Antarctic
798 phytoplankton species to ocean acidification: Growth, carbon acquisition, and
799 species interaction, *Limnol. Oceanogr.*, 58, 997–1007, 2013.
- 800 Von Caemmerer, S. V., and Farquhar, G. D.: Some relationships between the
801 biochemistry of photosynthesis and the gas exchange of leaves, *Planta*, 153, 376–
802 387, 1981.
- 803 WMO.: Greenhouse gas bulletin: The state of greenhouse gases in the atmosphere based
804 on global observations through 2012. World Meteorological Organization,
805 Geneva, Switzerland, ISSN 2078–0796, 2013.
- 806 Wawrik, B., Paul, J. H., and Tabita, F. R.: Real-time PCR quantification of *rbcL*
807 (ribulose-1,5-bisphosphate carboxylase/oxygenase) mRNA in diatoms and
808 pelagophytes, *Appl. Environ. Microbiol.*, 68, 3771–3779, 2002.
- 809 Welschmeyer, N. A.: Fluorometric analysis of chlorophyll *a* in the presence of
810 chlorophyll *b* and pheopigments, *Limnol. Oceanogr.*, 39, 1985–1992, 1994.
- 811 Wright, S. W., and van den Enden, R. L.: Phytoplankton community structure and
812 stocks in the east Antarctic marginal ice zone (BROKE survey, January–March
813 1996) determined by CHEMTAX analysis of HPLC pigment signature, *Deep-Sea*
814 *Res. II*, 47, 2363–2400, 2000.
- 815 Xu, H. H., and Tabita, F. R.: Ribulose-1,5-bisphosphate carboxylase/oxygenase gene
816 expression and diversity of lake Erie planktonic microorganisms, *Appl. Environ.*
817 *Microbiol.*, 62, 1913–1921, 1996.
- 818 Yoshimura, T., Nishioka, J., Suzuki, K., Hattori, H., Kiyosawa, H., Watanabe, Y.:
819 Impacts of elevated CO₂ on organic carbon dynamics in nutrient depleted Okhotsk
820 Sea surface waters, *J. Exp. Mar. Biol. Ecol.*, 395, 191–198, 2010.
- 821 Yoshimura, T., Sugie, K., Endo, H., Suzuki, K., Nishioka, J., and Ono, T.: Organic
822 matter production response to CO₂ increase in open subarctic plankton
823 communities: Comparison of six microcosm experiments under iron-limited
824 and-enriched bloom conditions, *Deep-Sea Res. I*, 94, 1–14, 2014.
- 825 Yoshimura, T., Suzuki, K., Kiyosawa, H., Ono, T., Hattori, H., Kuma, K., and Nishioka,
826 J.: Impacts of elevated CO₂ on particulate and dissolved organic matter

827 production: Microcosm experiments using iron deficient plankton communities in
828 open subarctic waters, *J. Oceanogr.*, 69, 601–618, 2013.

829 **Table 1.** Carbonate chemistry, nutrients, and Fe parameters (value \pm 1 standard
830 deviation, $n = 3$) during the incubation experiment. Carbonate parameters are the initial
831 and mean values throughout the incubation. Macronutrients and Fe parameters are the
832 values at the initial or final sampling days (i.e., day 5 for the control and day 6 for the
833 Fe-added treatments). Standard deviation was not assessed for initial TD-Fe
834 concentration because samples were collected from single source. See figures S1 and S2
835 for the complete data set.
836

	DIC ($\mu\text{mol kg}^{-1}$)	TA ($\mu\text{mol kg}^{-1}$)	$p\text{CO}_2$ (μatm)	CO_2 ($\mu\text{mol kg}^{-1}$)	pH (Total scale)
C-Initial	2086.4 \pm 2.8	2249.1 \pm 5.0	388.4 \pm 18.1	18.4 \pm 0.9	8.05 \pm 0.02
C-380	2075.5 \pm 8.1	2252.9 \pm 10.8	355.7 \pm 34.7	16.8 \pm 1.6	8.09 \pm 0.04
C-600	2151.6 \pm 7.8	2250.9 \pm 4.7	604.1 \pm 36.2	28.5 \pm 1.7	7.88 \pm 0.02
Fe-Initial	2085.3 \pm 0.8	2250.0 \pm 4.9	383.4 \pm 12.6	18.1 \pm 0.6	8.06 \pm 0.01
Fe-180	1959.9 \pm 62.0	2244.1 \pm 16.0	202.0 \pm 50.9	9.5 \pm 2.4	8.21 \pm 0.10
Fe-380	2068.5 \pm 27.7	2235.7 \pm 14.9	375.9 \pm 47.9	17.8 \pm 2.3	8.01 \pm 0.05
Fe-600	2120.6 \pm 33.5	2248.5 \pm 12.0	512.6 \pm 135.5	24.2 \pm 6.4	7.96 \pm 0.11
Fe-1000	2200.2 \pm 12.6	2248.4 \pm 9.8	913.8 \pm 159.8	43.2 \pm 7.6	7.72 \pm 0.07

837
838 **Table 1.** (Continued)
839

	Nitrate ($\mu\text{mol L}^{-1}$)	Phosphate ($\mu\text{mol L}^{-1}$)	Silicic acid ($\mu\text{mol L}^{-1}$)	TD-Fe (nmol L^{-1})
C-Initial	18.06 \pm 0.10	1.47 \pm 0.01	16.95 \pm 0.12	1.35
C-380	7.09 \pm 0.27	0.65 \pm 0.02	0.28 \pm 0.05	0.27 \pm 0.03
C-600	12.01 \pm 0.27	0.98 \pm 0.02	3.04 \pm 0.32	0.29 \pm 0.04
Fe-Initial	18.09 \pm 0.11	1.47 \pm 0.01	16.90 \pm 0.12	5.50 \pm 0.10
Fe-180	0.13 \pm 0.04	0.10 \pm 0.01	0.66 \pm 0.09	4.60 \pm 0.19
Fe-380	0.09 \pm 0.00	0.12 \pm 0.04	0.50 \pm 0.01	4.48 \pm 0.12
Fe-600	0.08 \pm 0.00	0.10 \pm 0.00	0.50 \pm 0.01	4.34 \pm 0.08
Fe-1000	0.08 \pm 0.00	0.08 \pm 0.02	0.47 \pm 0.02	4.18 \pm 0.24

840

841 **Table 2.** Number of OTUs, richness index, and diversity indices (value \pm 95%
 842 confidence interval) for *rbcL* cDNA libraries obtained from the initial seawater and the
 843 incubation bottles on day 2 (Fe-380 and Fe-600) and day 3 (C-380 and C-600).
 844

Library	No. of sequences	No. of OTUs	Chao1	H'	D
Initial	35	10	25.0	1.81 \pm 0.32	0.197 \pm 0.086
C-380	50	15	20.0	1.98 \pm 0.36	0.232 \pm 0.110
C-600	50	14	29.0	1.60 \pm 0.41	0.369 \pm 0.148
Fe-380	50	13	23.0	2.24 \pm 0.23	0.116 \pm 0.042
Fe-600	50	12	19.5	2.01 \pm 0.26	0.158 \pm 0.053

845

846 **Table 3.** Significance levels for differences among *rbcL* cDNA libraries as calculated
 847 with LIBSHUFF. *p* values < 0.05 are bolded.
 848

	Library (Y)				
	Initial	C-380	C-600	Fe-380	Fe-600
Library (X)					
Initial	—	0.434	0.573	0.383	0.587
C-380	0.153	—	0.086	0.101	0.898
C-600	0.523	0.500	—	0.004	0.033
Fe-380	<0.001	<0.001	<0.001	—	0.002
Fe-600	0.009	0.004	<0.001	0.030	—

849

850 **Figure captions**

851

852 **Figure 1.** Temporal changes in fucoxanthin (a and b) and 19'-hexanoyloxyfucoxanthin
853 (c and d) concentrations. Left (a and c) and right graphs indicate data from
854 the control and Fe-added treatments, respectively. Error bars denote ± 1
855 standard deviation (SD, $n = 3$). Standard deviations were not assessed on
856 days 2 (Fe-added treatments) and 3 (control treatments) because samples were
857 collected from each single bottle.

858

859 **Figure 2.** Mean contributions of each phytoplankton group to total Chl *a* biomass
860 estimated by CHEMTAX in the (A) control bottles at 380 and 600 ppm CO₂,
861 and (B) Fe-added bottles at 180, 380, 600 and 1000 ppm CO₂ ($n = 1$ or 3).

862

863 **Figure 3.** Relationship between fucoxanthin concentration and diatom-specific *rbcL*
864 copy number ($y = 7.62 \times 10^8 x + 1.90 \times 10^8$, $r^2 = 0.677$, $p < 0.001$, $n = 28$).

865

866 **Figure 4.** Abundances of *rbcL* mRNA (cDNA) normalized to *rbcL* gene copy number
867 (*rbcL* cDNA/DNA) in the control bottles on day 3 and the Fe-added bottles
868 on day 2. Open bars and closed bars denote control and Fe-added treatments,
869 respectively. Error bars indicate ± 1 SD ($n = 3$).

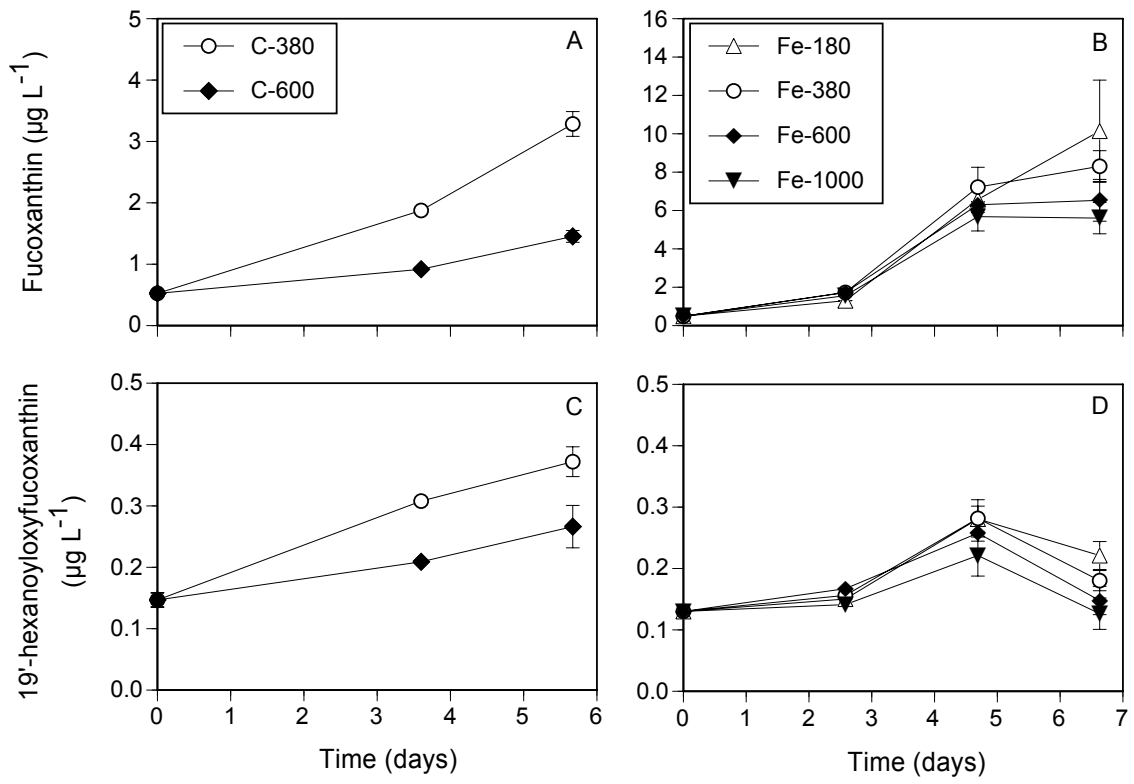
870

871 **Figure 5.** Rarefaction analysis of the diatom-specific *rbcL* clone libraries. The
872 rarefaction curves, plotting the number of operational taxonomic units
873 (OTUs) as a function of the number of sequences, were computed by the
874 software mothur. C and Fe indicate the control and Fe-added treatments,
875 respectively.

876

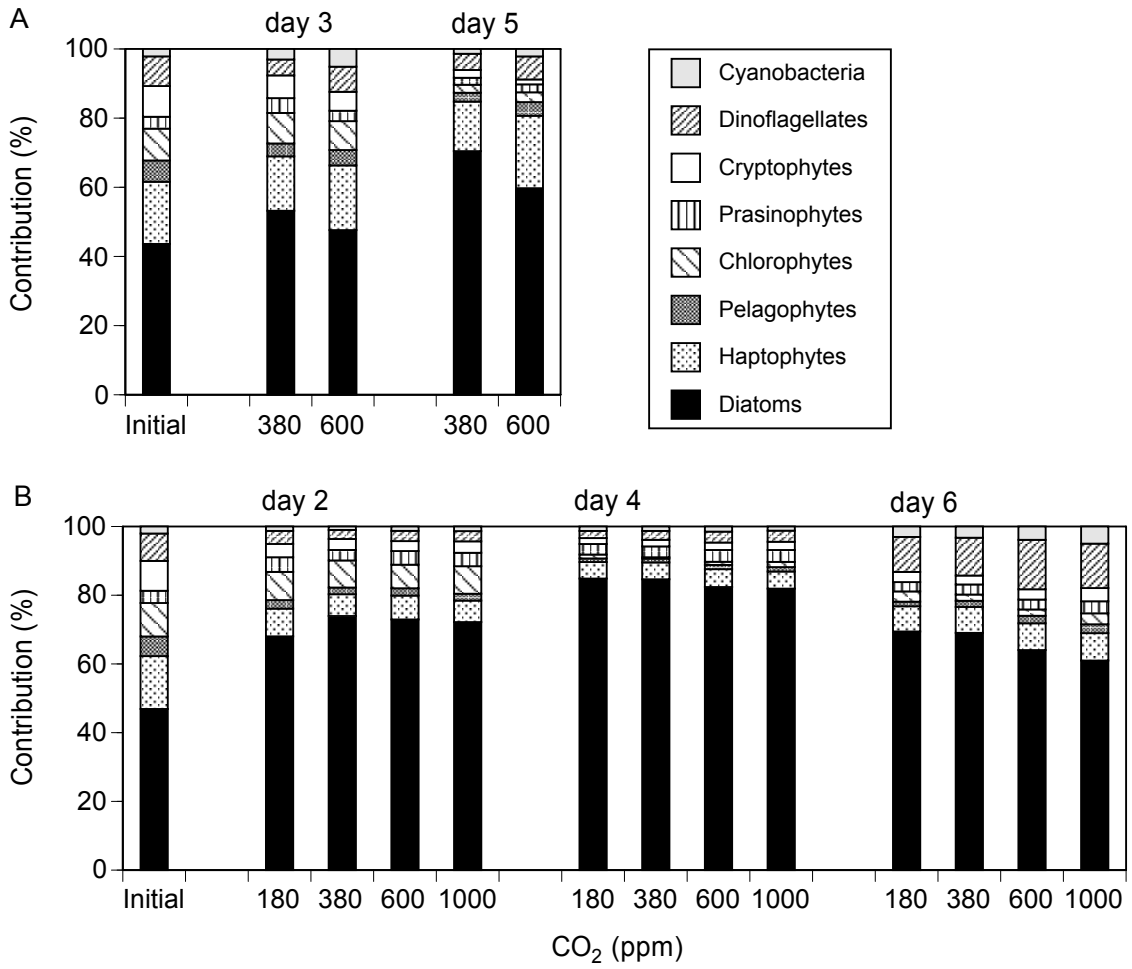
877 **Figure 6.** Relative phylotype contributions in the *rbcL* cDNA libraries obtained from
878 the initial seawater and the incubation bottles at day 2 (Fe-380 and Fe-600)
879 and day 3 (C-380 and C-600).

880



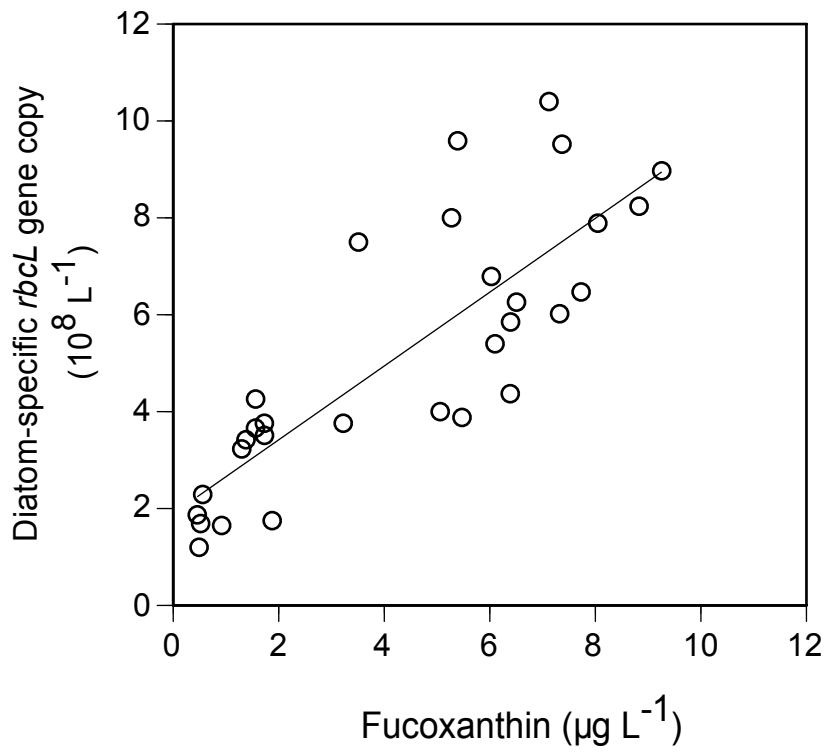
881

882 **Figure 1**



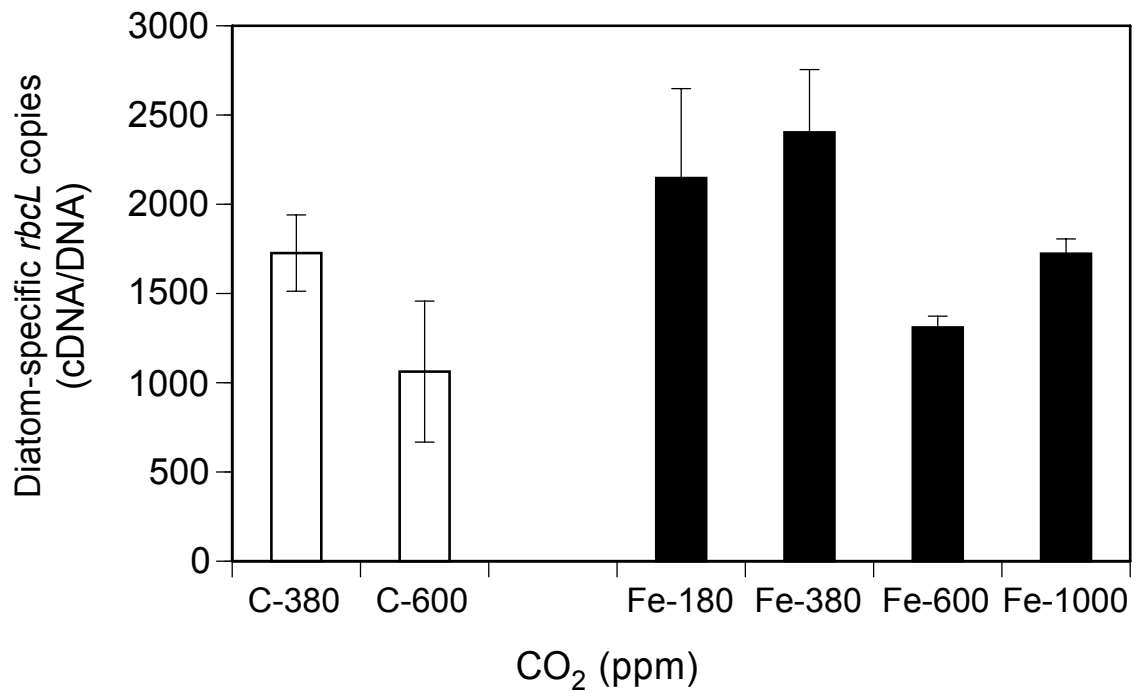
883

884 **Figure 2**



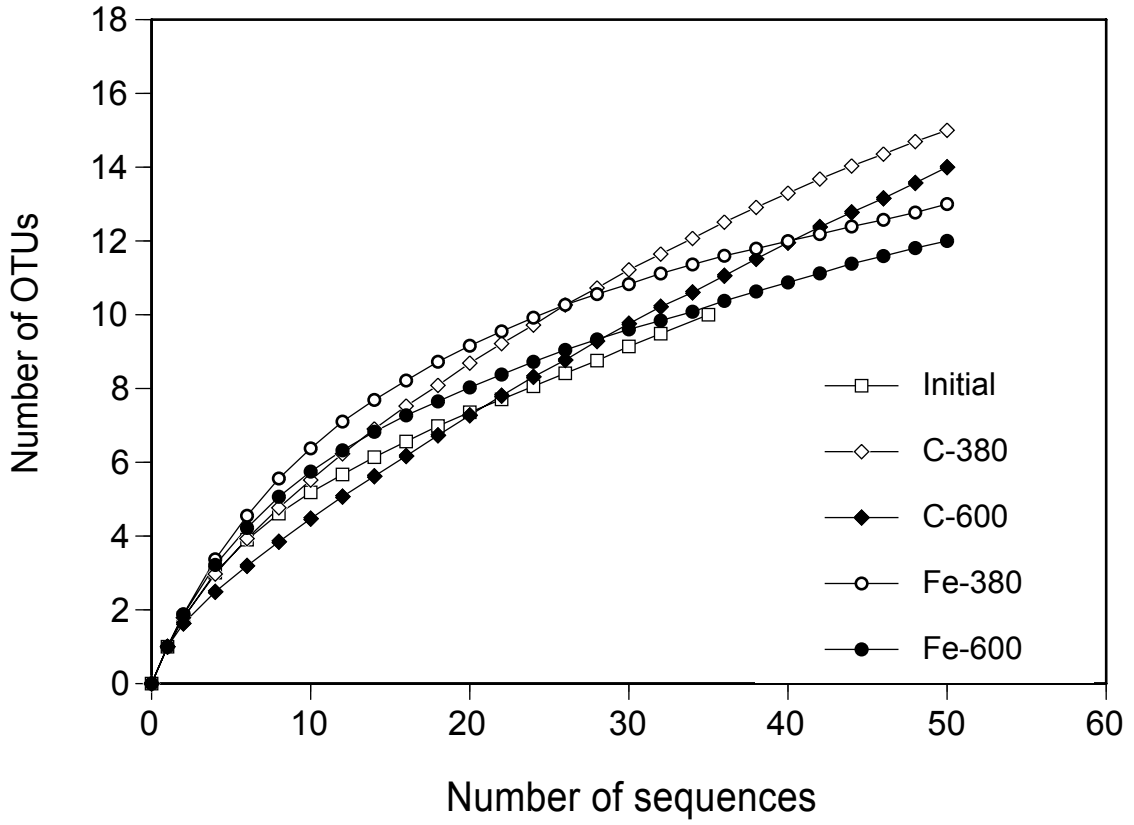
885

886 **Figure 3**



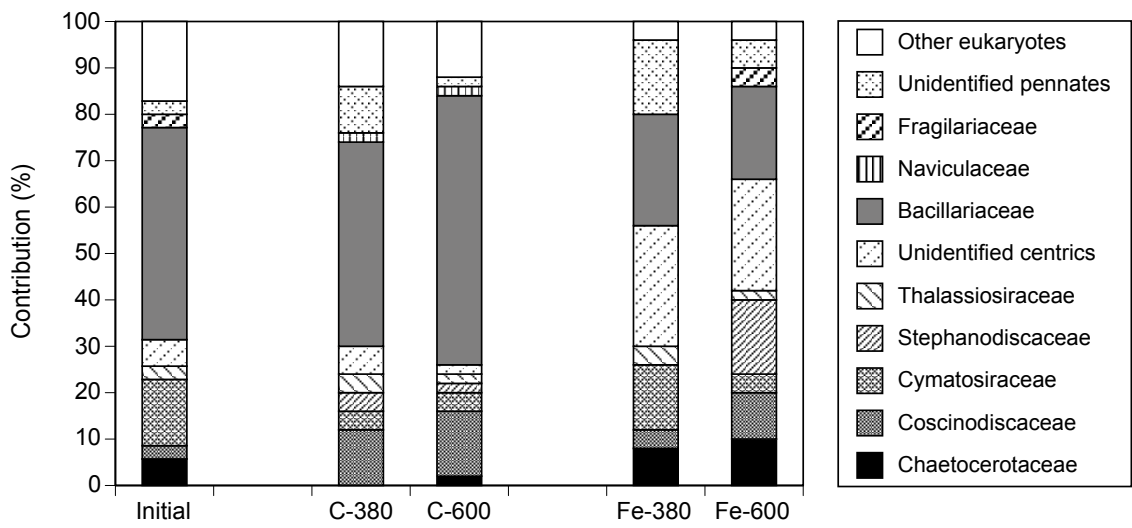
887

888 **Figure 4**



889

890 **Figure 5**



891

892 **Figure 6**